Null-plane phenomenology for the pion decay constant and radius

T. Frederico* and G. A. Miller
Department of Physics FM-15, University of Washington, Seattle, Washington 98195
(Received 9 September 1991)

The pion decay constant and the electromagnetic form factor are computed by using quark diagrams and projecting the bound-state wave function on the null plane. We show that the resulting formulas are the same as those of the Hamiltonian front-form scheme. The connection between the radius (r_π) and the pion decay constant (f_π) is studied using different models of confinement.

PACS number(s): 14.40.Aq, 12.40.Qq, 13.40.Fn

I. INTRODUCTION

The relativistic description of mesonic bound states is motivated, in part, by the desire to study the connection between the high-momentum component of the quark wave function and the corresponding long-range or short-wave length part of it. The problem of obtaining a physically reasonable relativistic wave function is extremly difficult and largely unsolved. Here we are concerned with understanding some simple first steps. One such description is obtained by making a truncation such as using only $\bar{q}q$ components, expressing the wave function in the null plane and evaluating a chosen graph. For example, one may evaluate the triangle diagram to obtain the elastic form factor [Fig. 1(a)]. (We consider only $\bar{q}q$ components of the wave function in our calculations, and one of our conclusions is that other components are necessary.) We define this procedure of using the null-plane wave function to evaluate a Feynman diagram the "diagrammatic approach."

The justification for the choice of variables in the null plane comes from the suppression of the pair creation or Z terms [1] in the amplitudes for specific processes after the integration over the null-plane energy. The calculation of form factors using the triangle diagram has been extensively discussed [1]. We generalize this procedure to calculate other observables by studying the π weak decay matrix element using the one-loop diagram of Fig. 1(b).

In the calculation of electromagnetic form factors using the triangle diagram, the plus component of the current, $J^+=J^0+J^3$, is used because it is a "good" operator [2] that does not create pairs. This is a symptom that such calculations are not complete. Indeed, rotational invariance is not completely respected.

Another apparently different approach was suggested long ago [3]. This approach, now called Hamiltonian front-form dynamics [1,4], continues [5,6] and was generalized to other pseudoscalar mesons [7,8]. It was used in the nuclear context, in particular, for the calculation of the deuteron form factors [1,4,9].

In Hamiltonian front-form dynamics, the null-plane wave function is constructed as an eigenfunction of the mass operator and its kinematical dependence on the null-plane coordinates is easily obtained [1,4,10]. The separation of the center-of-mass coordinate is also straightforward. The null-plane bound-state wave function is written as a function of the transverse relative momentum p_t and the fraction of momentum $x=p^+/P^+$, where p^+ corresponds to the momentum of that of the constituents and P^+ is the plus component of the total momentum. The connection with the usual nonrelativistic wave function comes when the third component of the relative momentum of the two nucleons is defined from the free mass operator of the two-body system. The most important difference between the relativistic and nonrelativistic approaches comes from the coupling of the angular momentum and spin. The coupling is carried out in the c.m. frame in the instant form and reexpressed in terms of light-cone spinors [11]; this relates the front form of the Clebsch-Gordan coefficients [1,4] with the Melosh rotation. The null plane is defined by $x^+=x^0+x^3=0$. We use the metric and Dirac spinors defined by Bjorken and Drell [12].

The formulation of the Hamiltonian front form of the dynamics can also be understood as a special choice for the kinematical operators [13,14] from among the generators of the Poincaré group. These operators define the subgroup of the Poincaré group, which leaves the null plane invariant. This means that among the 10 generators of the Poincaré group, the maximal number of seven

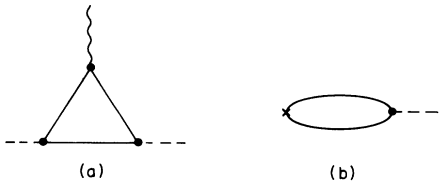

FIG. 1. One-loop diagrams for (a) the electromagnetic form factor (triangle diagram) and (b) the pion decay constant.

*Permanent address: Instituto de Estudos Avançados, Centro Técnico Aerospacial, 12225 São José dos Campos, São Paulo, Brazil.

are chosen as independent of the interaction [13]. The remaining three dynamical operators, which contain the interaction, can be constructed from the mass operator and the three components of the spin operator rotated by a Melosh transformation [15].

Reference [1] showed that the elastic electromagnetic form factors of a bound state computed from the triangle diagram and from the Hamiltonian front-form dynamics are the same. The integration in the momentum loop over the null-plane energy in the plus component of the current is the essential step. The Melosh transformation is then seen to result from using the Feynman fermion propagator.

Thus the "diagrammatic approach" and Hamiltonian front-form dynamics are two relativistic techniques available for computing observables. The results for the elastic form factors are the same, but it is not yet known if such an equality holds for other observables. We shall compare computations of the π weak decay constant, f_π for the two procedures.

An apparently completely different third approach is to use the soft-pion limit. The pion radius and weak decay constant are related by $\langle r_\pi^2 \rangle^{1/2} = \sqrt{3}/2\pi f_\pi$ [16]. This is a result of the integration of the triangle diagram for a $\pi - \bar{q}q$ vertex independent of momentum. The essential physics is contained in the triangle diagram, and because the radius is the derivative of the form factor, the one-loop integral is convergent even with a constant vertex, thus relating r_π and f_π. The Nambu–Jona-Lasinio model also yields this result [17].

So a question arises: does the null-plane phenomenology destroy the remarkable relation between r_π and f_π? We try to answer this question by performing several numerical calculations in the perspective of the connection between these two quantities for different models of the pion wave function.

The plan of the paper is as follows. In Sec. II we evaluate the one-loop diagrams for the pion electromagnetic form factor and weak decay constant. It turns out that the results obtained from the diagrammatic approach for the form factor and f_π are the same as those of light-cone quantum mechanics or Hamiltonian front-form dynamics. In Sec. III, the numerical results for r_π and f_π for different models in the null plane are given and compared with the soft-pion limit. A summary of our new numerical results is given in Sect. IV.

II. ONE-LOOP DIAGRAMS FOR THE FORM FACTOR AND DECAY CONSTANT

The pion electromagnetic form factor is calculated from the triangle diagram of Fig. 1(a), and the weak decay constant is obtained from the one-loop diagram with the weak vertex $\gamma^\mu\gamma^5$, as shown in Fig. 1(b). The $\pi \to \bar{q}q$ vertex is determined by implementing the physics of spontaneous breaking of chiral symmetry. To fix the conventions for the pion and to obtain the vertex describing the $\pi \to \bar{q}q$ process, we present a brief review.

The pion viewed as the Goldstone boson arising from the spontaneous breaking of chiral symmetry has many rich consequences in low-energy hadronic phenomenology. For a review see Ref. [18]. The first striking feature of the pion is the small mass compared to other hadrons. This comes naturally in the Goldstone picture as is shown in the Gell-Mann, Oakes, and Renner [19] relations for the masses of pseudoscalar mesons. The interactions between the quarks spontaneously breaks chiral symmetry. Because the interaction Lagrangian is invariant under the chiral transformation, only the free Lagrangian is necessary for obtaining the coupling of the Goldstone boson with the quarks. Then, we start by making a chiral rotation in the free Lagrangian:

$$\mathcal{L} = \bar{q}(i\partial\!\!\!/ - \hat{m})q \ , \tag{1}$$

where $\hat{m}$ is the average between the up and down bare quark masses.

The chiral angle is associated with the pion field, and the quark field rotated by the chiral transformation

$$q' = \exp\left[i\frac{\boldsymbol{\pi}\cdot\boldsymbol{\tau}\gamma^5}{2f_\pi} \right] q \ . \tag{2}$$

Here the pion field operator $\boldsymbol{\pi}$ is an elementary field.

The couplings of the pion field with the quarks are taken from the Lagrangian after the chiral transformation of the quark field, and the quark gets the constituent mass M from the spontaneous breaking of chiral symmetry. The couplings of the pion to the quark field are obtained by the expansion of the chiral rotation. Then, we keep terms up to first order in the pion field and in the second order for the scalar term $(\bar{q}q)$. This gives

$$\mathcal{L} = \bar{q}(i\partial\!\!\!/ - M)q - \frac{1}{2f_\pi}\partial_\mu \boldsymbol{\pi}\cdot\bar{q}\gamma^\mu\gamma^5\boldsymbol{\tau}q - i\frac{\hat{m}}{f_\pi}\boldsymbol{\pi}\cdot\bar{q}\gamma^5\boldsymbol{\tau}q + \frac{\hat{m}}{2f_\pi^2}\pi^2\bar{q}q \ . \tag{3}$$

The quark field operators q' are written as q in Eq. (3) and in the following text. Keeping only the terms of Eq. (3) is consistent with our stated approximation of keeping only $\bar{q}q$ components of the pion wave function.

The second term in the Lagrangian gives the pseudoscalar coupling of the pion to the quarks, when the constituent mass is used for the quark. This is the Goldberger-Treiman [20] relation at the quark level. If the effects of spontaneous symmetry breaking dominate the pion wave function, it is a good approximation to take $i\partial\!\!\!/ q = Mq$ with M the constituent quark mass. Then the interaction Lagrangian $\mathcal{L}_1$ for the $\pi \to \bar{q}q$ vertex is given by

$$\mathcal{L}_1 = -i(M/f_\pi)\boldsymbol{\pi}\cdot\bar{q}\gamma^5\boldsymbol{\tau}q \ . \tag{4}$$

This has the form of a $\pi \to \bar{q}q$ coupling with a constant vertex function. The third term of Eq. (3) has the same form as this one, but is neglected because the bare quark mass is small.

The third term gives the Gell-Mann, Oakes, and Renner relation for m_π,

$$m_\pi^2=\frac{\hat{m}}{f_\pi^2}\langle 0|\bar{q}q|0\rangle\ , \tag{5}$$

and the scalar vacuum condensate of quarks is the measure of chiral-symmetry breaking.

The general structure of the $\bar{q}q$ bound state of the pion comes from the pseudoscalar coupling, and we will use such spin structure in the following discussion of the one-loop diagrams.

A. Pion electromagnetic form factor

We choose to work in the Breit frame where the momentum transfer is such that $q^+=0$ and $q_\perp=(q_x,0,0)$ to make contact with the null plane impulse approximation of the pion form factor [6]. The triangle diagram for the pion electomagnetic current is

$$e(p^\mu+p'^\mu)F(q^2)=\langle\pi^+|J^\mu|\pi^+\rangle$$
$$=ie2\frac{M^2}{f_\pi^2}N_c\int\frac{d^4k}{(2\pi)^4}\,\mathrm{tr}\left[\frac{\not k+M}{k^2-M^2-i\epsilon}\gamma^5\frac{\not k-\not p'+M}{(k-p')^2-M^2-i\epsilon}\gamma^\mu\frac{\not k-\not p+M}{(k-p)^2-M^2-i\epsilon}\gamma^5\right], \tag{6}$$

where $p^0=p'^0$ and $\mathbf{p}'_\perp=-\mathbf{p}_\perp=\mathbf{q}_\perp/2$ in the Breit frame. $N_c=3$ is the number of colors.

The plus component of the current is calculated, because in general the k^- integration is convergent. This property is essential for the null-plane phenomenology.

We evaluate the integral of Eq. (6) by performing the integration over k^- first. This yields an expression which can be interpreted as involving spatial pion wave functions that depend on the plus and $\perp$ components of the $\bar{q}q$ relative momentum. Proceed by changing the variables from $k^\mu=(k^0,\mathbf{k})$ to $(k^-=k^0-k^3,\ k^+=k^0+k^3,\mathbf{k}_\perp)$ and performing the trace. Then one obtains

$$F(q^2)=i\frac{M^2}{f_\pi^2}4N_c\int\frac{dk^+d^2k_\perp dk^-}{(2\pi)^4}\frac{2(k-p)^+\left[k_\perp^2+M^2-\frac{k^-}{2}(k-p)^+\right]-k^+\left[k_\perp^2+M^2-\frac{q_\perp^2}{4}\right]}{k^+(k^+-p^+)^2\left[k^--\frac{k_\perp^2+M^2+i\epsilon}{k^+}\right]}$$
$$\times\frac{1}{\left[k^--p^--\frac{(k_\perp-p_\perp)^2+M^2+ie}{k^+-p^+}\right]}\frac{1}{\left[k^--p^--\frac{(k_\perp-p'_\perp)^2+M^2+i\epsilon}{k^+-p^+}\right]}\ , \tag{7}$$

where the singularity structure in the k^- integration is explicitly shown.

The integral over k^- is convergent, and one can apply the Cauchy theorem. There are three distinct situations that must be analyzed: $k^+<0$, $0<k^+<p^+$, and $k^+>p^+$. The first and the third regions of k^+ integration do not contribute to the integral because the three poles have imaginary parts with the same sign. The only contribution comes from the region of $0<k^+<p^+$. This corresponds to the spectator quark in the photon absorption process to be on-mass shell. So its plus component of the momentum cannot exceed that of the pion. The result is

$$F(q^2)=\frac{2}{(2\pi)^3}\frac{M^2}{f_\pi^2}N_c\int\frac{dx\,d^2K_\perp}{x(1-x)}M_0^2\times\frac{1+\frac{(1-x)\mathbf{q}_\perp\cdot\mathbf{K}_\perp}{K_\perp^2+M^2}}{(m_\pi^2-M_0^2)(m_\pi^2-M'^2_0)}\ , \tag{8}$$

where the momentum fraction $x=(p^+-k^+)/p^+$ and $0<x<1$. The relative perpendicular momentum is defined as [1,3–10]

$$\mathbf{K}_\perp=(1-x)(\mathbf{p}_\perp-\mathbf{k}_\perp)-x\mathbf{k}_\perp\ , \tag{9}$$

and $\mathbf{K}'_\perp=\mathbf{K}_\perp+(1-x)\mathbf{q}_\perp$. The free mass operator for the $q-\bar{q}$ is written in terms of the momentum fraction and the relative perpendicular momentum,

$$M_0^2=\frac{K_\perp^2+M^2}{x(1-x)}\ , \tag{10}$$

and M'_0 is written as a function of $K'_\perp$.

The integration of Eq. (7) can be used to obtain the pion radius $r_\pi^2=-(1/6)dF/dq^2|_{q=0}$. In the soft-pion limit ($m_\pi=0$), Eq. (8) gives the well-known result of $\langle r_\pi^2\rangle^{1/2}=\sqrt{3}/2\pi f_\pi$ from Ref. [16]. The null-plane integration gives the correct result for r_π that could not be achieved using the bad (other than plus) components of the current.

The next step is to interpret Eq. (8), in terms of an integral involving spatial pion wave functions Φ_π. Note

Eq. (8) is obtained using a constant pion-$\bar{q}q$ vertex function. The structure of the standard Drell-Yan formula for the form factor emerges from Eq. (8) if one interprets the denominators as wave functions. In particular,

$$\Phi_\pi \sim \frac{1}{-m_\pi^2+M_0^2} . \tag{11}$$

This is a standard expression for a wave function, obtained using a constant vertex function. The other factors in the integrand of Eq. (8) arise from the Melosh rotation of the spin wave function of the quarks, as shown below.

The next step is to use a more realistic model for Φ_π. This will be done by modifying the vertex function. A necessary preliminary is to discuss the normalization factors. It turns out to be useful to make another change of variables $(x,K_\perp)\to\mathbf{K}$ to rewrite Eq. (8). This also helps us to make contact with the null-plane impulse approximation as given by the Hamiltonian front form of the dynamics [4,6]. The Jacobian of the transformation is

$$\frac{\partial(x,K_\perp)}{\partial(K_z,K_\perp)} = 4\left[\frac{[x(1-x)]^3}{K_\perp^2+M^2}\right]^{1/2} , \tag{12}$$

and

$$K_z = \left[x-\frac{1}{2}\right]\left[\frac{K_\perp^2+M^2}{x(1-x)}\right]^{1/2} . \tag{13}$$

The normalization condition of the pion wave function is that $F(q^2=0)=1$. Using the new variables, this is

$$1 = \frac{N_c}{\pi^3}\frac{M^2}{f_\pi^2}\int d^3K \frac{M_0}{(-m_\pi^2+M_0^2)(-m_\pi^2+M_0^2)} . \tag{14}$$

We require that $\Phi_\pi(K)$ is normalized to unity, so that one may identify the wave function in terms of the relative coordinates as

$$\Phi_\pi(K) = \frac{1}{\pi^{3/2}}\frac{M}{f_\pi}\frac{\sqrt{M_0 N_c}}{-m_\pi^2+M_0^2} . \tag{15}$$

Using the above expression for the wave function in Eq. (8) leads to

$$F(q^2) = \int d^3K \left[\frac{M_0}{M_0'}\right]^{1/2}\left[1+\frac{(1-x)\mathbf{q}_\perp\cdot\mathbf{K}_\perp}{K_\perp^2+M^2}\right] \times\Phi_\pi(K')\Phi_\pi(K) . \tag{16}$$

Our expression (16) for the pion form factor is the same as that obtained in Ref. [6] using Hamiltonian front-form dynamics.

In the numerical work presented below, the expression (15) for the pion wave function is modified to include the effects of a nonconstant vertex function. This is done by using different phenomenological forms for Φ_π. Such forms include the effects of confinement. It is interesting to see if the soft-pion relation between r_π and f_π is maintained. Thus we compute the pion decay constant using a similar triangle diagram analysis.

B. Pion weak decay constant

The pion decay constant is calculated from PCAC (partial conservation of axial-vector current) [20] which is expressed through the diagram in Fig. 1(b)

$$p_\mu \langle 0|\bar{q}\gamma^\mu\gamma^5\tau_i q|\pi_j\rangle = 2ip^2 f_\pi \delta_{ij} , \tag{17}$$

where $f_\pi = 93$ MeV.

Using Eq. (4) for the pion-$\bar{q}q$ vertex function, one obtains

$$ip^2 f_\pi = N_c\frac{M}{f_\pi}\int\frac{d^4k}{(2\pi)^4}\,\mathrm{tr}\left[\not{p}\gamma^5\frac{\not{k}-M}{k^2-M^2-i\epsilon}\times\gamma^5\frac{\not{p}-\not{k}-M}{(p-k)^2-M^2-i\epsilon}\right] . \tag{18}$$

Our aim here is to integrate over k^- in order to obtain an expression for f_π written as an integral involving a pion wave function expressed on the null plane. So, performing the Dirac algebra, and separating the poles in the k^- plane, one obtains

$$f_\pi^2 = 2iM^2N_c\int\frac{dk^+d^2k_\perp dk^-}{(2\pi)^4 k^+(p^+-k^+)}\frac{1}{\left[k^- - \frac{k_\perp^2+M^2+i\epsilon}{k^+}\right]\left[p^- - k^- - \frac{k_\perp^2+M^2+i\epsilon}{p^+-k^+}\right]} . \tag{19}$$

We evaluate this expression in the pion rest frame. The integral over k^- is convergent, and only values of k^+ such that $0<k^+<p^+$ contribute. The result is

$$f_\pi^2 = 2N_c\frac{M^2}{(2\pi)^3}\int\frac{dx\,d^2k_\perp}{x(1-x)}\frac{1}{-m_\pi^2+\frac{k_\perp^2+M^2}{x(1-x)}} . \tag{20}$$

The expression for f_π in the constant vertex elementary pion field approach can be generalized by again using the replacement suggested in Eq. (15). The final equation is

$$f_\pi = \frac{M\sqrt{N_c}}{4\pi^{3/2}}\int\frac{dx\,d^2K_\perp}{x(1-x)}\frac{\Phi_\pi(K)}{\sqrt{M_0}} . \tag{21}$$

This is the same expression found by Chung, Ji, and Cotanch [8] obtained using Hamiltonian front-form dynam-

ics. Thus, the expressions for the weak decay constant and the electromagnetic form factor are the same for each of the two formulations we consider. This emphasizes the role played by the elementary Feynman diagrams in the interpretation of the null-plane phenomenology.

Note that Eqs. (14) [or (8) with $q^2=0$] and (20) provide independently obtained different expressions for f_π. Our numerical work shows that the two expressions yield similar results. This can be traced to the fact that if one takes the soft-pion limit, Eq. (8) with $q^2=0$ and Eq. (20) yield the same expression for f_π.

III. NUMERICAL RESULTS

We perform numerical calculations using three wave functions: (i) a Gaussian, in which the main characteristic is confinement; (ii) an hydrogen-atom type that mimics one-gluon exchange at short distances; and (iii) the pion wave function model of Ref. [21]. This last wave function has the effects of (iterated) one-gluon exchange and confinement.

In order to define the transformation of the c.m. wave function to the null-plane variables, one needs to specify the mass of the quark in the calculations. We choose the constituent quark masses

$$M=330 \text{ MeV} , \tag{22}$$

and

$$M=220 \text{ MeV} . \tag{23}$$

This last value is used to compare the results of the hydrogen and Gaussian models to those obtained from Ref. [21]. The pion model of Ref. [21] uses a quark-mass (M) of 220 MeV, which we do not vary.

The hydrogen-atom and the Gaussian model wave functions depend only on one range parameter that can be related to the nonrelativistic radius. The nonrelativistic radius is defined as

$$r_{\rm NR}=-\frac{1}{6}\frac{dF_{\rm NR}}{dq^2} , \tag{24}$$

and

$$F_{\rm NR}(q^2)=\int d^3K\,\Phi_\pi\left(\left|\mathbf{K}+\frac{\mathbf{q}}{2}\right|\right)\Phi_\pi(K) . \tag{25}$$

We display the ratio of the pion radius to the nonrelativistic radius as a function of $r_{\rm NR}$ in Fig. 2. Two different masses $M=330$ and 220 MeV are used. The results do not depend very much on the model wave function once the constituent quark mass is fixed. It is important to note that in each case the true or measured radius increases over the nonrelativistic one [6]. This difference is caused by the Melosh rotation of the spins. (Equivalently, one could say the difference is caused by the use of a Feynman propagator for the intermediate fermions.) As one would expect, the relative increase in the radius over the nonrelativistic one is pronounced for smaller values of $r_{\rm NR}$. This helps in the phenomenology of the nonrelativistic quark model, where the radius of the mesons is naively computed to be much smaller than the experimental values [21].

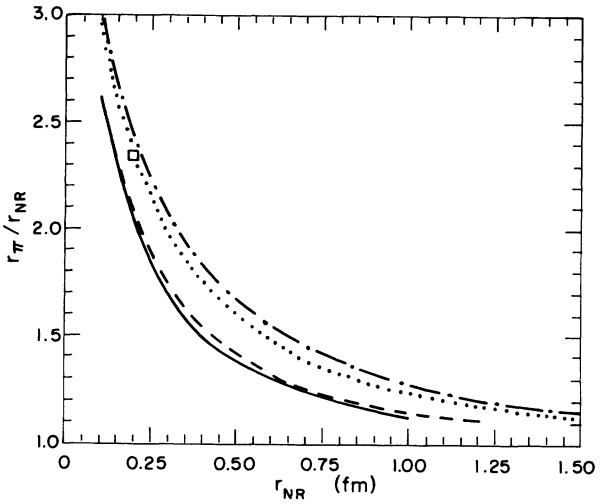

FIG. 2. Ratio of the pion radius to the nonrelativistic radius as a function of the nonrelativistic radius of the model wave function. Hydrogen-atom model (solid line) and Gaussian model (dashed line) for $M=330$ MeV. Hydrogen-atom model (dotted line) and Gaussian model (dot-dashed line) for $M=220$ MeV [(square) Ref. [21]].

Our calculation is only concerned with the quark core of the pion, but in the context of the vector-dominance model this core could be much smaller than the observed radius [17]. Even with the relativistic increase of r_π the computed r_π is smaller than the data (0.66±0.07) [22], and the computed value of f_π is much larger than the measurements. Perhaps one should include effects of the virtual mesons ($\pi\to\rho\pi$) or other non-$\bar{q}q$ components. This has not yet been done in the context of the null-

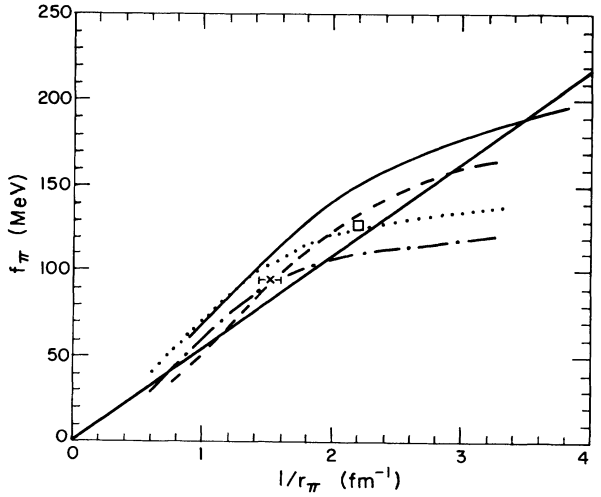

FIG. 3. Pion weak decay constant as a function of r_π^{-1}. The curves are labeled as in Fig. 2. The soft-pion limit $f_\pi=\sqrt{3}/2\pi r_\pi$ is the straight solid line. The data point, indicated by ×, is that of Ref. [22].

TABLE I. $r_\pi(fm)$ and f_π(MeV) for different models, the nonrelativistic radius is 0.195 fm for all the cases. The pion model of Ref. [21] gives $r_\pi=0.456$ fm and $f_\pi=123.0$ MeV in the null-plane phenomenology.

	H atom		Gaussian	
M (MeV)	r_π	f_π	r_π	f_π
100	0.606	63.98	0.612	56.01
220	0.463	124.5	0.476	108.2
300	0.408	156.4	0.422	135.7
400	0.361	188.7	0.375	162.1

plane phenomenology.

In Fig. 3, we plot the results of f_π as a function of $(r_\pi)^{-1}$. The limiting case of the soft-pion limit of the triangle diagram using a constant vertex function is shown as the solid line through the origin. This can be compared to the results obtained with our three model wave functions. The experimental data point is also shown. For larger r_π there is model independence. However, the three models yield different results for small pion sizes. The inverse relationship between r_π and f_π is approximately valid for the Gaussian and hydrogen models. If the core of the pion is small, the corresponding f_π will be greater than the experimental value, unless a constituent quark mass smaller than usual is chosen.

In Table I, we show the results for the hydrogen and Gaussian models for different quark masses and a fixed nonrelativistic radius of 0.195 fm. This is the value quoted in Ref. [21] for the pion wave function. The results follow the qualitative behavior given by the soft-pion limiting formula. The model dependence for the radius is small, as we already observed from Fig. 2.

IV. SUMMARY

The diagrammatic approach is applied to compute the form factor and weak decay constant of the pion. We show that the diagrammatic approach gives the same results as Hamiltonian front-form dynamics.

We study numerically the pion electromagnetic radius and weak decay constant for different models (Ref. [21], Gaussian and hydrogen atom) of the $q-\bar{q}$ pion wave function. The connection between the values of r_π and f_π is examined. The computed pion radius is independent of the model, once the constituent quark mass and nonrelativistic radius is fixed.

The results suggest that the soft-pion limit of the triangle diagram for the pion radius and decay constant is also approximately obtained by the null-plane calculations for different models. In the case of a small $q\bar{q}$ core of the pion our results show that the experimental value of the pion decay constant cannot be easily reproduced in null-plane calculations. One possibility is to invoke gluonic and multiquark degrees of freedom in the pion wave function [23], and from that the pion decay constant will be renormalized, because the probability of the $q\bar{q}$ component is not equal to unity. This means that further studies of the pion wave function are needed.

ACKNOWLEDGMENTS

One of us (T.F.) would like to acknowledge useful discussions with S. Cotanch, L. L. Frankfurt, and M. I. Strikman. This work was supported in part by the Conselho Nacional de Desenvolvimento Científico e Tecnológico—(CNPq), Fundação de Amparo à Persquisa do Estado de São Paulo—FAPESP, Brazil and the U.S. Department of Energy.

[1] L. L. Frankfurt and M. I. Strikman, Nucl. Phys. **B148**, 107 (1979); Phys. Rep. **76**, 215 (1981).

[2] R. Dashen and M. Gell-Mann, in *Proceedings of the 3rd Coral Gables Conference on Symmetry Principles at High-Energy,* 1966, edited by A. Perlmutter (Freeman, San Francisco, 1967); S. Fubini, G. Segré, and D. Walecka, Ann. Phys. (N.Y.) **39**, 381 (1966); V. de Alfaro, S. Fubini, G. Furlan, and C. Rossetti, *Currents in Hadron Physics* (North-Holland, Amsterdam, 1973).

[3] M. V. Terent'ev, Yad. Fiz. **24**, 207 (1976) [Sov. J. Nucl. Phys. **24**, 106 (1976)].

[4] P. L. Chung, F. Coester, B. D. Keister, and W. N. Polyzou, Phys. Rev. C **37**, 2000 (1988).

[5] Z. Dziembowski, Phys. Rev. D **37**, 778 (1988), and references therein.

[6] P. L. Chung, F. Coester, and W. N. Polyzou, Phys. Lett. B **205**, 545 (1988).

[7] I. G. Aznauryan and K. A. Oganesyan, Yad. Fiz. **47**, 1731 (1988) [Sov. J. Nucl. Phys. **47**, 1097 (1988)]; Phys. Lett. B **249**, 309 (1990).

[8] C. R. Ji and S. Cotanch, Phys. Rev. D **21**, 2319 (1990); S. Cotanch (private communication); C. R. Ji, P. L. Chung, and S. Cotanch, following paper, Phys. Rev. D **45**, 4214 (1992).

[9] I. L. Grach and L. A. Kontratyuk, Yad. Fiz. **39**, 316 (1984) [Sov. J. Nucl. Phys. **39**, 198 (1984)]; L. L. Frankfurt, I. L. Grach, L. A. Kondratyuk, and M. Strikman, Phys. Rev. Lett. **62**, 387 (1989); T. Frederico, G. A. Miller, and E. M. Henley, Nucl. Phys. **A533**, 617 (1991); M. I. Strikman, L. L. Frankfurt, and T. Frederico, University of Washington Report No. 40427-21-N91 (unpublished).

[10] B. L. G. Bakker, L. A. Kondratyuk, and M. V. Terent'ev, Nucl. Phys. **B158**, 497 (1979); L. A. Kontratyuk and M. V. Terent'ev, Yad. Fiz. **31**, 1087 (1980) [Sov. J. Nucl. Phys. **31**, 361 (1980)].

[11] J. M. Namyslowski, Prog. Part. Nucl. Phys. **14**, 49 (1985).

[12] J. D. Bjorken and S. D. Drell, *Relativistic Quantum Fields* (McGraw-Hill, New York, 1965).

[13] P. A. M. Dirac, Rev. Mod. Phys. **21**, 392 (1949).

[14] H. Leutwyler and J. Stern, Ann. Phys. (N.Y.) **112**, 94 (1978).

[15] H. J. Melosh, Phys. Rev. D **9**, 1095 (1974).

[16] R. Tarrach, Z. Phys. C **2**, 221 (1979).

[17] V. Bernard and U. G. Meissner, Phys. Rev. Lett. **61**, 2296 (1988).

[18] U. G. Meissner, Phys. Rep. **161**, 213 (1988), and references

therein.
[19] M. Gell-Mann, R. J. Oakes, and B. Renner, Phys. Rev. **175**, 2195 (1968).
[20] C. Itzykson and J. B. Zuber, *Quantum Field Theory* (McGraw-Hill, New York, 1980).
[21] S. Godfrey and N. Isgur, Phys. Rev. D **32**, 189 (1985).
[22] S. R. Amendolia *et al.*, Phys. Lett. B **178**, 435 (1986).
[23] G. P. Lepage and S. J. Brodsky, Phys. Rev. D **22**, 2175 (1980).